Mon. Not. R. Astron. Soc. **000**, 1–4 (2013) Printed 22 January 2014 (MN LATEX style file v2.2)

Hydrodynamics associated to the X-ray light curve of A0620-00

Y. Coronado, S. Mendoza⋆
Instituto de Astronomía, Universidad Nacional Autónoma de México, AP 70-264, Distrito Federal 04510, México

arXiv:1401.5395v1 [astro-ph.HE] 21 Jan 2014

22 January 2014

ABSTRACT
From 1975 to 1976, an outburst was detected in the light curve of the X-ray transient A0620-00 using the Ariel V and SAS-3 experiments. In this letter we model the outburst with the hydrodynamical model proposed by Mendoza et al. (2009). The physical model is constructed assumming basic mass and momentum conservation laws associated to the motion of the shock waves developed inside the expanding relativistic jet of the source. These internal shock waves are produced as a result of periodic variations of the inyected mass and velocity of the flow at the base of the jet. The observations of this X-ray light curve present two clear bumps. The first one is modelled assuming periodic variations of the inyected velocity at the base of the jet, while the second one can either be modelled by a further velocity oscillations, or by a periodic variation of the mass injection rate at the base of the jet at a latter time. The fitting of the data fixes different parameters of the model, such as the mean mass injection rate at the base of the jet and the oscillation frequency of the flow as measured on the rest frame of the central source.

Key words: – Relativistic Jets – Relativistic Hydrodynamics – microquasar

1 INTRODUCTION

On August 3rd, 1975 the low-mass X-ray binary black hole transient A0620-00, exhibited its most powerful outburst detected by the Sky Survey Experiment on board the Ariel V satellite in X-rays (Elvis et al. 1975). On August 8th, this micro-quasar was also followed by the SAS-3 X-ray observatory (Matilsky et al. 1976). Subsequently it was also seen in different wavelengths, from radio to ultraviolet (see Kuulkers 1998, for a review). At that time, A0620-00 became the most powerful X-ray source in the sky for almost two months.

Five days after the discovery of A0620-00 intense variations on time scales of days, which reached a maximum value ~ 50 times that of the Crab Nebula in the energy interval of $1.5 - 6$ KeV, suggested that the source was an an excellent candidate for a stellar mass black hole with a stellar companion. This idea was further corroborated by the direct observations made by McClintock & Remillard (1986) which resolved the binary components of the source. The estimated distance to A0620-00 is ~ 1Kpc (Shahbaz et al. 1994), being one of the nearest X-ray transients objects, hosting a black hole with a mass function $f(m) = 3.18 \pm 0.16\, M_{\odot}$ (McClintock & Remillard 1986; Marsh et al. 1994).

Using dynamical and stellar numerical models, the inclination of the accretion disc with respect to the orbit spanned by the black hole and the stellar companion yields $i = 51^{\circ} \pm 0.9$, implying a black hole mass $6.6 \pm 0.25\, M_{\odot}$, and an estimated distance to the source 1.06 ± 0.12 Kpc (Cantrell et al. 2010).

The radio emission of A0620-00 was detected in 1975 (Davis et al. 1975; Owen et al. 1976a), with no jet resolved. Since many X-ray transient systems containing a black hole have radio emission that follows their X-ray outburst with clear detections of relativistic outflows or jets (Abdo et al. 2009), it was clear that a jet should have been produced in the X-ray outburst of A0620-00. Kuulkers et al. (1999) infered the existance of that jet by compiling different radio observations, concluding that the speed of the jet $\sim 0.9c$, where c is the velocity of light.

In this letter, we assume that the mechanism producing the observed light curve of A0620-00 is caused by variations in the injected flow at the base of the jet, which leads to the formation of shock waves that propagate along the jet. The hydrodynamical jet model presented in Mendoza et al. (2009, hereafter M09) describes the motion of working surfaces inside a relativistic jet, which are able to fit the observed light curves of long gamma-rays bursts (lGRBs) as well as the light curve of the blazar PKS 1510-089 (Cabrera et al. 2013). The shape of the X-ray light curve of the micro-quasar A0620-00 is similar to the one observed in lGRBs, showing an exponential rapid increase

⋆ E-mail address: coronado@astro.unam.mx, sergio@astro.unam.mx.

© 2013 RAS

with a slow decay. With all these, the the physical ingredients of the phenomena that produces the light curve of A0620-00 can be considered similar to those ones ocurring in lGRB and on PKS 1510-089, but with different physical scales of energy, sizes, masses, accretion power rates, etc. (Mirabel & Rodriguez 2002).

The letter is organised as follows. In Section 2 we present the X-ray data of the light curve of A0620-00. In Section 3 we briefly describe the main features of the hydrodynamic model by M09, and using that model we fit the observational data in Section 4. Finally, the results of our fits and the discussion of the main physical parameters inferred by the modelling are presented in Section 5.

2 OBSERVATIONAL DATA

The observational 1975-1976 X-ray light curve of the micro-quasar A0620-00 is shown in Figure 1 and was kindly provided by Jeffrey McClintock. It consist of a composition of two independent lightcurves obtained by Elvis et al. (1975) and Matilsky et al. (1976), with instruments on board Ariel V and SAS-3 respectively. Both data count-rates have been converted to flux Crab units, according to the instruments specifications (Whitlock et al. 1992). With this it is possible to get a complete light curve of the 1975-1976 outburst, including a bump in the decaying outburst. Figure 1 shows the plotted data on a linear scale, with the advantage of revealing the impressive outburst of 1975 and a clear second bump a few days after the maximum. To convert from Crabs to mJy, we use the conversion given by Kirsch et al. (2005) and Bradt et al. (1979) for the Ariel V data (in the energy range $1-13$ KeV) and the one in `http://heasarc.gsfc.nasa.gov/docs/sas3` for the SAS-3 satellite (in the energy range $2-10$KeV). This conversion is coherent with the results obtained by Kirsch et al. (2005), for which $1\mathrm{Crab} \approx 2.4\times10^{-11}\mathrm{Wm}^{-2}$ in the energy range $1-13$KeV.

In order to calculate the Luminosity L we multiply the obtained Flux F by $4\pi D^2\delta^{-p}$, where $\delta := 1/\Gamma(v_0)(1-(v_0/c)\cos\theta)$. For this particular case, since the inclination angle $i \approx 51^\circ$, then the angle θ between the jet and our line of sight is $\approx 39^\circ$, with a distance to the source $D = 1\,\mathrm{Kpc}$ (Owen et al. 1976b; Shahbaz et al. 1994; Cantrell et al. 2010). The beaming index p for synchrotron radiation is 3 (Longair 2011) and we have chosen such value in accordance to the calculations of blazars and lGRBs (Wu et al. 2011; Mendoza et al. 2009; Cabrera et al. 2013), having in mind a unified radiative model for the flow inside all relativistic astrophysical jets. With this luminosity, and with the average jet bulk speed of $v_0 = 0.9c$ (Kuulkers et al. 1999), we are able to fit the observational data with the hydrodynamical model of M09.

Attempts to model the light curve of A0620-00 were made by Kuulkers et al. (1999) who noticed that this behaviour might well be understood modelling many "*synchrotron bubble*" ejections. Since micro-quasars are thought to be short scaled versions of quasars and are thus logical scaled counterparts of lGRB (Mirabel & Rodriguez 2002), it is quite natural to model their behaviour using the model by M09 to model their light curve. We thus assume that velocity and mass variations at the base of the jet of the micro-quasar A0620-00 produce internal shock waves that travel inside the expanding relativistic jet and that these shock waves in turn are able to reproduce its observed light curve.

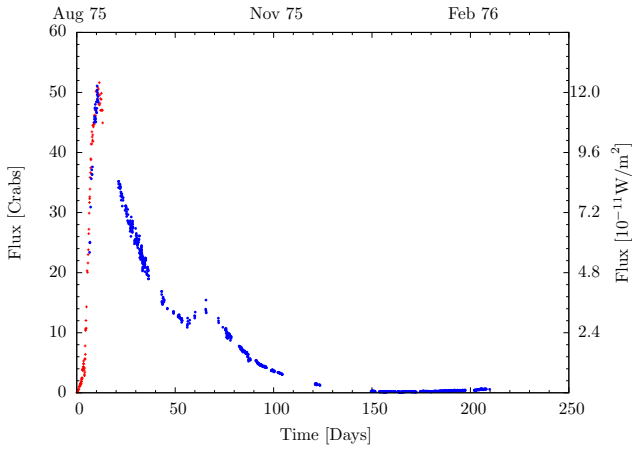

Figure 1. The figure shows the X-ray light curve of the micro-quasar A0620-00. The crossess correspond to the Ariel V observations, which covers the uprise of the curve and the beginning of its decay. The points are SAS-3 observations, which cover the first outburst and the bump at the decaying of the burst.

3 THE HYDRODYNAMICAL MODEL.

Many relativistic jets show internal shock waves, which are due to the interaction of the jet with inhomogeneities of the surrounding medium (see e.g Mendoza & Longair 2001), the bending of jets (see e.g Mendoza & Longair 2002) and time fluctuations in the velocity and mass of the ejected material (cf. Rees & Meszaros 1994; Jamil et al. 2008; Mendoza et al. 2009). In particular the semi-analytical model of M09 is a hydrodynamical description of time fluctuations at the base of the jet that develop shock waves inside an expanding relativistic jet.

The model of M09 produce internal shock waves by periodic oscillations of speed and mass discharge at the base of the jet. This mechanism injects fast fluid that overtakes slow one, producing an initial discontinuity which eventually forms a working surface expanding along the jet. The extra kinetic energy inside the working surface is thus radiated away. The efficiency converting factor between kinetic energy and observed radiation is assummed to be ~ 1. This value was used by M09 and Cabrera et al. (2013) for lGRBs and the Blazar PKS1510-089. We have made such a choice, since a micro-quasar can be considered as a scaled version of a quasar. Furthermore, A0620-00 has been the most energetic X-ray micro-quasar and in this sense shares the same behaviour as PKS1510-089 which presented extreme γ-ray energy detections. As explained in Section 1, the micro-quasar A0620-00 behaves as an scaled typical lGRB and as such, the hypothesis used by M09 can be extended to this particular object. As we will discuss in section 5, this assumption yields physical parameters which are coherent with the expectations of typical micro-quasars.

Following M09, we assume that the flow is injected at the base of the jet with a periodic velocity v given by:

$$v(\tau) = v_0 + c\eta^2 \sin\omega\tau, \quad (1)$$

and a periodic mass injection rate:

$$\dot{m}(\tau) = \dot{m}_0 + \epsilon^2 \sin\Omega\tau, \quad (2)$$

where τ is the time measured in the proper frame of the source, the velocity v_0 is the "average" velocity of the flow inside the jet, and ω is the oscillation frequency of the flow. The positive constant parameters η^2 and ϵ^2 are obtained by fitting the observational data, with the particular feature that η^2 has to be sufficiently small so that the bulk velocity $v(\tau)$ does not exceed the velocity of light c. The mass injection rate $\dot{m}_0$ is the "average" discharge of the flow at the base of the jet, and Ω is its oscillation frequency.

4 MODELLING THE X-RAY LIGHT CURVE

As previously discussed, the first outburst resembles the light curve of a typical lGRB. As such, we model that burst by assuming $\dot{m} = $ const., in complete accordance to the calculations by M09. The bump in the decay of the first burst is modelled in two ways. The first is by assuming a new ejection with constant discharge added up to the first outburst. The second way is by assuming an oscillating mass discharge $\dot{m}$ produced at a particular time while the first outburst decays.

In the first burst, where $\dot{m} = $ const., the semi-analytical model presented by M09, requires to know the values of v_0, η^2, ω and $\dot{m}$. The "mean" velocity value v_0 can be taken from observational data. For this particular case, we choose the inferred value from a wide variety of radio observations modelled through ejection mechanisms by Kuulkers et al. (1999) which yields a Lorentz factor $\Gamma(v_0) = 2.3$. Since the value of η^2 has to be small due to the expected variations inside the jet, we start with a small value of η^2 such that the bulk velocity of the flow $v(\tau = 0) \sim 0.1 \times v_0$. The velocity variations $v(\tau)$ are thus allowed to vary from this value up to the extreme upper limit $\Gamma(v(\tau)) \sim 10$. As pointed by M09, the mass ejection rate is related to the observed luminosity $L = \dot{m}c^2$ and is obtained directly from the fits of the light curve.

The second burst can be described by two different mechanisms: (a) The mass discharge $\dot{m}$ is kept constant and the velocity is the sum of the velocity as in equation (1) with an extra oscillating term $\eta'^2 \sin\omega'\tau$, with the same v_0, η^2 and ω used for the callibration of the first outburst. (b) The velocity is the same as the one used for the callibration of the first burst, and the mass discharge $\dot{m}$ is allowed to oscillate as in equation (2), with $\dot{m}_0$ given by the results obtained with the callibration of the first outburst.

Following Cabrera et al. (2013), we set a dimensionless system of units to perform the required fitting. To do so, the luminosity is measured in units of the peak luminosity and the time in units of the FWHM of each particular outburst. This system of units is such that for the first outburst $\omega = 1$ and $\dot{m} = 1$, with the only unknown η^2 obtained by a linear regression analysis to within 10% of accuracy. For the case of the second outburst: (a) The only unknown is η'^2 obtained with a further linear regression analysis. (b) The unknown quantity is ϵ^2 which can be obtained by another regression analysis. To return to the physical system of units one can recall at any particular step that the luminosity $L = \dot{m}c^2$ (for the first outburst) and that the time $t = \omega^{-1}\tau$ (case (a) of the second outburst), $t = \omega'^{-1}\tau$ and $t = \Omega^{-1}\tau$ (case (b) of the second outburst).

1st. outburst

η^2/c 10^{-3}	ω 10^{-2}d	$\dot{m}$ $10^{-9}M_\odot \mathrm{yr}^{-1}$	$\Gamma_{\max}$
1.679	6.6	2.8063	2.31

2nd. outburst - case (a)

η'^2/c 10^{-3}	ω' 10^{-2}d	$\dot{m}$ $10^{-9}M_\odot \mathrm{yr}^{-1}$	$\Gamma_{\max}$
0.061	249.1	0.8391	3.61

2nd. outburst - case (b)

ϵ^2/c $10^{-9}M_\odot \mathrm{y}^{-1}$	Ω 10^{-2}d	$\dot{m}$ $10^{-9}M_\odot \mathrm{yr}^{-1}$	$\Gamma_{\max}$
0.8959	1.5	0.7466	2.31

Table 1. Obtained values for the free parameters of the model by M09 after fitting with X-ray observations of the light curve of the micro-quasar A062-00, accurate to within 10%. The background Lorentz factor of the bulk velocity of the flow was assumed to be 2.29. The maximum Lorentz factor of the flow in each outburst is represented by $\Gamma_{\max}$, and the minimum is $\sim 1.8 - 2.2$.

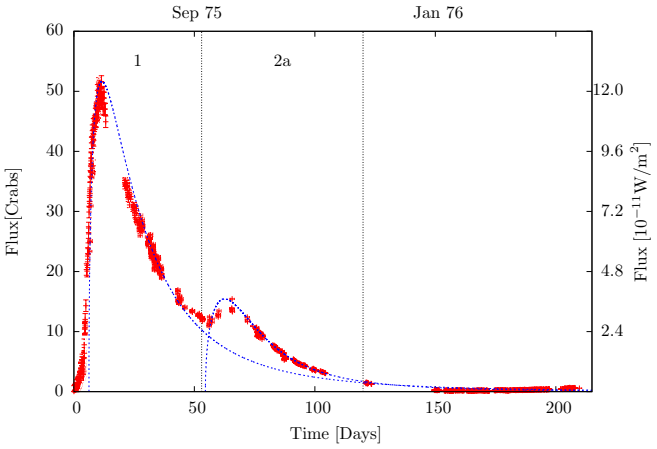

Figure 2. The figure shows the fits to the X-ray light curve observations of the micro-quasar A0620-00, which corresponds to velocity variations and constant mass discharges for the first and second outburst (model (a) -see text). The second outburst has an additional oscillating velocity component as compared to the first one.

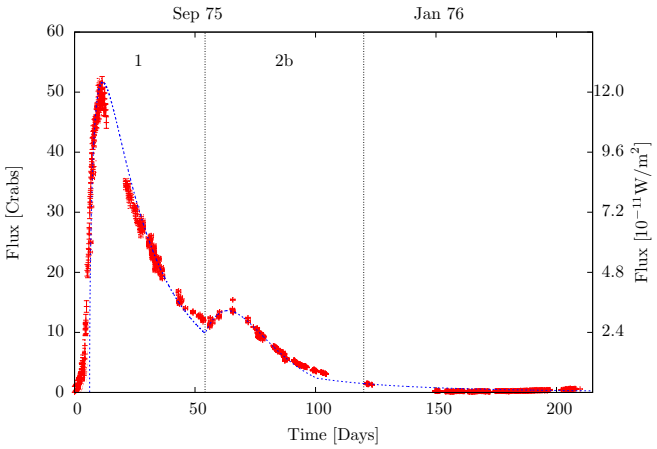

Figure 3. The figure shows the fits to the X-ray light curve observations of the micro-quasar A0620-00, which corresponds to velocity variations for the first and second outburst, but with constant mass discharge at the first outburst and oscillating mass discharge at the second outburst (model (b) -see text).

5 DISCUSSION

The results of the fits to the X-ray data presented in Section 2 using the model by M09 are shown in Figures 2 and 3. The obtained values for the physical parameters of the model are presented in Table 1. We have also included the maximum and minimum Lorentz factors, obtained for the bulk velocity of the flow. Direct inspection on the results of the Table show that $\dot{m} \sim 10^{-9} - 10^{-10} \mathrm{M}_{\odot}\mathrm{yr}^{-1}$, $\omega^{-1} \sim 0.01-2$ days with a maximum Lorentz factor 2.3−3.6.

A00620-00 resulted to be an ideal target to test the model by Mendoza et al. (2009) since it closely resembles a lGRB in this outstanding outburst in x-rays. Future tests of the model have to be done with a wide variety of Light Curves from a large collection of micro-quasars.

6 ACKNOWLEDGMENTS

The authors gratefully acknowledge the kindness of Jeffrey E. McClintock for providing the observational data and for pointing to the relevant articles discussing those observations. This work was supported a DGAPA-UNAM grant (PAPIIT IN111513-3). YUC and SM thank support granted by CONACyT: 210965 and 26344.

REFERENCES

Abdo A. A. et al., 2009, Science, 323, 1688
Bradt H. V., Doxsey R. E., Jernigan J. G., 1979, in Baity W. A., Peterson L. E., eds, X-ray Astronomy. pp 3–66
Cabrera J. I., Coronado Y., Benítez E., Mendoza S., Hiriart D., Sorcia M., 2013, MNRAS, 434, L6
Cantrell A. G. et al., 2010, ApJ, 710, 1127
Davis R. J., Edwards M. R., Morison J., Spencer R. E., 1975, Nature, 257, 659
Elvis M., Page C. G., Pounds K. A., Ricketts M. J., Turner M. J. L., 1975, Nature, 257, 656
Jamil O., Fender R. P., Kaiser C. R., 2008, in Microquasars and Beyond.
Kirsch M. G. et al., 2005, in Siegmund O. H. W., ed., Society of Photo-Optical Instrumentation Engineers (SPIE) Conference Series Vol. 5898, UV, X-Ray, and Gamma-Ray Space Instrumentation for Astronomy XIV. pp 22–33
Kuulkers E., 1998, New Astronomy Reviews, 42, 1
Kuulkers E., Fender R. P., Spencer R. E., Davis R. J., Morison I., 1999, MNRAS, 306, 919
Longair M. S., 2011, High Energy Astrophysics
Marsh T. R., Robinson E. L., Wood J. H., 1994, MNRAS, 266, 137
Matilsky T. et al., 1976, ApJL, 210, L127
McClintock J. E., Remillard R. A., 1986, ApJ, 308, 110
Mendoza S., Hidalgo J. C., Olvera D., Cabrera J. I., 2009, MNRAS, 395, 1403
Mendoza S., Longair M. S., 2001, MNRAS, 324, 149
Mendoza S., Longair M. S., 2002, MNRAS, 331, 323
Mirabel I. F., Rodriguez L. F., 2002, Sky and Telescope, 103, 050000
Owen F. N., Balonek T. J., Dickey J., Terzian Y., Gottesman S. T., 1976a, ApJL, 203, L15
Owen F. N., Balonek T. J., Dickey J., Terzian Y., Gottesman S. T., 1976b, ApJL, 203, L15
Rees M. J., Meszaros P., 1994, ApJL, 430, L93
Shahbaz T., Naylor T., Charles P. A., 1994, MNRAS, 268, 756
Whitlock L., Lochner J., Rhode K., 1992, Legacy, 2, 25
Wu Q., Zou Y.-C., Cao X., Wang D.-X., Chen L., 2011, ApJL, 740, L21